Advances in Science and Technology Research Journal

Advances in Science and Technology Research Journal, 2025, 19(5), 96–112
https://doi.org/10.12913/22998624/200594
ISSN 2299-8624, License CC-BY 4.0

Received: 2024.11.26
Accepted: 2025.03.14
Published: 2025.04.01

Application of metaheuristic algorithms for optimisation of brake force distribution in agricultural trailers

Zbigniew Kamiński[1]

[1] Faculty of Mechanical Engineering, Department of Machine Design and Exploitation, Bialystok University of Technology, Wiejska Str. 45C, 15-351 Bialystok, Poland
E-mail: z.kaminski@pb.edu.pl

ABSTRACT

According to EU Regulation 2015/68 on the approval of agricultural vehicles, high-speed trailers of categories R3 and R4 must meet the brake force distribution requirements between the axles. Five metaheuristic algorithms (MIDACO, Cuckoo Search, Firefly Algorithm, Simulated Annealing, and Harmony Search) implemented in open-source MATLAB code were used to optimize the linear brake force distribution found in trailers with braking force regulators. The optimization results obtained for a two-axle and a three-axle trailer with two variants of tandem axles (bogie and two leaf springs) are very close to the results obtained by the Quasi-Monte Carlo method. Although metaheuristic methods do not always guarantee that an exact optimum solution will be found, they can be successfully applied to the selection of brake force distribution in the initial stages of brake system design. They have the advantage of flexibility, simplicity, less mathematical complexity, and avoidance of local optima. The brake force distribution optimization results can be used to establish the parameters of the wheel braking mechanisms of agricultural trailer axles.

Keywords: agricultural trailer, brake force distribution; optimization; metaheuristic method.

INTRODUCTION

In terms of road safety, the braking systems of agricultural vehicles must comply with several requirements set out in EU Delegated Regulation 2015/68 [1]. These requirements concern, among other things, braking performance and high-speed operation under emergency braking (reaction time of less than 0.6 s) and tracking action during slow braking [2]. For trailers travelling at speeds above 30 km/h, a 50% braking performance requirement has been set for both air and hydraulic braking systems. In addition, trailers of categories R3, and R4 and towed agricultural machinery of category S2, i.e. with a gross mass of over 3500 kg and travelling at speeds of over 40 km/h, must comply with the prescribed distribution of braking forces between axles (groups of axles) and ensure compatibility with the braking systems of tractors [1].

To select the distribution of braking forces, Regulation [1] sets out the permissible limits of variation of the utilized adhesion rate of individual vehicle axles (ratio of braking force to normal ground reaction) from the ideal distribution as a function of the braking rate. As the provisions of [1] treat each part of the combination as a single vehicle, without taking into account the braking control of the towed vehicle, the permissible ranges of variation of the braking rate of both vehicles (expressing the ratio of the braking forces generated by the vehicle to its mass) have been defined for the tractor-trailer combination. A Compatibility is deemed to be met if the curve of the braking rate as a function of the control pressure at the coupling head, for both the laden and unladen trailer, falls within specified tolerance zones, known as “compliance bands” or “compliance corridors” [3].

Axle load transfer and brake force distribution (BFD) are key factors in road vehicle safety and stability [4], so the braking system design begins with BFD selection [5]. Braking force distribution is fundamental to the design calculations and selection of the basic components of vehicle brakes and has a significant impact on braking performance [6]. In general, for both unladen and laden vehicles, the best possible match to the ideal distribution is sought [7], while meeting the requirements of [1]. For an ideal BFD, the adhesion utilized by each axle is the same, that is each axle has the same ratio of brake force to its vertical load [8]. For semi-trailers, the ratio of longitudinal to vertical force on the coupling device of a towed vehicle is also the same [9]. Such a distribution is considered optimal as it maximizes braking efficiency and ensures braking stability [10].

Air and hydraulic braking systems for agricultural trailers often use manual or automatic braking force regulators with radial characteristics [11, 12], briefly described in section 4. This type of regulator provides a linear BFD between the front and rear axle(s) according to the vehicle load. The boundary and optimum parameters for the linear BFD of two-axle vehicles, including trailers, can be calculated by analytical methods [13]. Recently, optimization methods have been increasingly used to realize different BFD strategies for vehicles [14, 15]. Optimization methods are particularly useful for selecting the BFD on vehicles with tandem suspension [6]. In general, reaction moments during braking change the load distribution among the leading and trailing axles [16]. As load transfer between tandem axles can cause premature wheel lockup, the design of the tandem unit and the BFD between the axles have a clear influence on braking performance [17].

In this paper, metaheuristic optimization algorithms (MOAs) are used to search for the optimal linear BFD in agricultural trailers. MOAs have been developed based on the simulation of various natural phenomena, animal and human behaviour, biological and chemical sciences, physical concepts, game rules, and other evolutionary processes [18, 19]. Metaheuristic algorithms, one of the most widely used probabilistic methods, are highly effective in solving complex optimization problems. Metaheuristic algorithms work by using a random search mechanism in the problem space. The advantages of MOAs include the simplicity of their concepts, ease of implementation, independence from the specific problem type, and the ability to solve non-linear, non-convex, discontinuous, non-derivative, and high-dimensional optimization problems [20]. Metaheuristic algorithms, successfully complemented by constraint handling techniques [21], are applied to solve optimization problems in many fields, including artificial intelligence, business, science, and engineering [22, 23]. Optimization of the BFD of a two-axle and a three-axle trailer with two variants of the tandem unit was carried out using five different metaheuristic algorithms implemented in open-source MATLAB code. The results achieved were compared with those obtained using a quasi-Monte Carlo method. Although metaheuristics do not always guarantee the exact optimal solution but can lead to a computationally efficient near-optimal solution. An important advantage of metaheuristic algorithms in BFD optimization is the possibility to use their freely available implementations in MATLAB.

REQUIREMENTS FOR BRAKE FORCE DISTRIBUTION OF TRAILERS

Vehicle brake distribution affects braking behaviour, braking performance, and road safety [24]. To achieve good longitudinal braking performance of a tractor-trailer combination on a flat and level road, it is necessary to achieve as close as possible to an ideal braking distribution, while meeting the type-approval requirements, including the dynamic stability of the vehicle combination [25, 26].

Ideal braking condition is obtained when the adhesion utilized by each axle or group of front or rear axles (tandem, tri-axle) is equal to the braking rate z of the combination. For trailers with a group of axles, this condition can be expressed as follows:

$$f_1 = f_2 = f_{1i} = f_{2i} = z \; z = \frac{\sum T_{1i} + \sum T_{2i}}{\sum R_{1i} + \sum R_{2i}} \tag{1}$$

where: T_{1i}, R_{1i} – braking forces and axle loads in the front axle group, T_{2i} , R_{2i} – braking forces and axle loads in the rear axle group, i – axle number in the front or rear axle group, f_1, f_2 – utilized adhesion of front and rear group of axles:

$$f_1 = \frac{\sum T_{1i}}{\sum R_{1i}} \; f_2 = \frac{\sum T_{2i}}{\sum R_{2i}} \tag{2}$$

The BFD described by relation (1) is considered optimal because it minimizes stopping distance by allowing each axle to reach its maximum braking capability [27] and ensures braking performance [25].

Due to variations in the load status of trailers, it is virtually impossible to obtain an ideal BFD, even with load-sensing braking force regulators. For agricultural trailers travelling at speeds above 40 km/h, Regulation (EU) 2015/68 [1] therefore defines permissible limits for the departure of the adhesion utilization curve of individual axles (axle groups) from the ideal BFD.

When considering the BFD, each part of the vehicle combination is treated as a single vehicle. The forces at the coupling are not taken into account. Two acceptable solutions for trailers are shown in Figure 1.

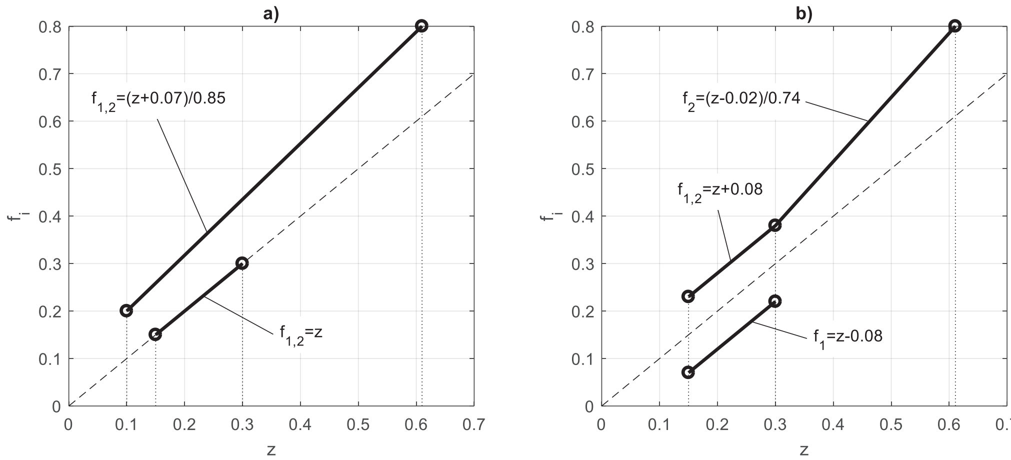

Figure 1. Limits of utilized adhesion according to EU Regulation 2015/68 [1]: a - first solution, b - second solution

First solution: the rate of adhesion utilisation of each axle group must satisfy the condition of required minimum braking performance:

$$f_{1,2} \leq \frac{z+0.07}{0.85} \text{ for } 0.1 \leq z \leq 0.61 \tag{3}$$

and prevents premature lockup of rear axle wheels to maintain directional stability:

$$f_1 > z > f_2 \text{ for } 0.15 \leq z \leq 0.30 \tag{4}$$

Second solution: the rate of adhesion utilisation of each axle group must lie within a range bounded by the following inequalities:

$$\begin{matrix} f_1 \geq z - 0.08 \\ f_{1,2} \leq z + 0.08 \end{matrix} \text{ for } 0.15 \leq z \leq 0.30 \tag{5}$$

Furthermore, the adhesion utilisation for the rear axle group should satisfy the constraint:

$$f_2 \leq \frac{z-0.02}{0.74} \text{ for } 0.30 \leq z \leq 0.61 \tag{6}$$

For a more accurate calculation, the divisor in (6) should be fixed at 0.7381.

The requirements for the wheel locking sequence shall be considered to be met if the adhesion utilized by the front axle is greater than the adhesion utilized by at least one of the rear axles at a braking rate ranging from 0.15 to 0.30. [1]:

$$f_1 > f_{2i} \text{ for any } i \tag{7}$$

METHOD FOR THE SELECTION OF THE OPTIMUM LINEAR BFD

To match the ideal BFD, several types of load-dependent brake force regulators are installed in the air braking systems of agricultural trailers. At present, automatic load sensing valves (LSV, ALB) are most commonly used on heavy trailers to adjust the brake pressure on the axles according to the load status [11]. If the brake distribution is designed correctly, this will prevent the wheels from locking up when the trailer is partially laden or unladen. On mechanically sprung trailers the adjustment is relative to the spring deflection, on air-sprung trailers it depends on the pressure of the air springs. If there are technical reasons against equipping the vehicles with an LSV (especially non-suspended vehicles), agricultural trailers or machines should be equipped with a manual brake force regulator. Due to the difficulty of meeting the requirements of EU 2015/68 for BFD on vehicles with manual three-stage adjustment (full - half - empty), BPW has developed a seven-stage mechanical load-dependent brake force regulator (MBL), but with a linear characteristic [28]. This means that the output pressure remains proportional to the control pressure. For hydraulic braking systems, manual and automatic load-sensing valves with radial characteristics have also been developed [12]. Since the characteristics of the pressure distribution of the MLB and ALB regulators are substantially straight lines, the BFD between the front and rear group of axles can also be regarded as linear.

An axle's braking contribution is the ratio of its partial braking force to the trailer's total braking force. Thus, for a three-axle tandem trailer, the BFD coefficients are defined as follows:

$$\beta_1 = \frac{T_1}{z \cdot G} \qquad \beta_2 = \frac{T_{2T}}{z \cdot G} \qquad \beta_{21} = \frac{T_{21}}{z \cdot G} \qquad \beta_{22} = \frac{T_{22}}{z \cdot G} \tag{8}$$

where: T_{2T} – total brake force of the tandem axles.

BFD coefficients can theoretically vary between 0 and 1 and satisfy the relationships:

$$\beta_1 + \beta_2 = 1 \qquad \beta_{21} + \beta_{22} = \beta_2 \tag{9}$$

Using equations (8) and (9) the brake forces of the front and tandem axles are calculated as follows:

$$T_1 = \beta_1 z \cdot G \qquad T_{2T} = (1 - \beta_1) z \cdot G \; T_{21} = \beta_{21} z \cdot G \; T_{22} = (1 - \beta_1 - \beta_{21}) z \cdot G \tag{10}$$

A directional coefficient of the BFD line crossing the origin of the coordinate system T_{2T}=f(T_1) is given as the brake force ratio:

$$i_P = \frac{T_{21} + T_{22}}{T_1} = \frac{T_{2T}}{T_1} \tag{11}$$

It is also possible to apply a linear braking distribution to tandem axles, either variable or fixed (if there is no braking force regulator):

$$i_S = \frac{T_{22}}{T_{21}} \tag{12}$$

Unlike the β coefficients, the i_P and i_S values can be theoretically varied from zero to infinity, especially when the brake force of some axle is zero.

The following 5 metaheuristic methods were used to optimize the BFD coefficients: MIDACO, Cuckoo Search, Firefly Algorithm from the group of swarm-based algorithms, Simulated Annealing from the group of physics and chemistry-based algorithms, and Harmony Search from the group of algorithms based on human intelligence. The primary criterion for the selection of these algorithms was the availability of their implementations in the MATLAB programming environment, and additionally in versions adapted to solve constrained optimization tasks. It should be remarked that the vast majority of publicly available MATLAB programs with examples of the application of metaheuristic methods deal with optimization problems without constraints.

The MIDACO software (Mixed Integer Distributed Ant Colony Optimisation) implements a global optimization algorithm for nonlinear programming problems using an extended ACO algorithm [29] coupled with the Oracle penalty method [30] for handling constraints. This advanced and universal penalty method requires only one parameter to be tuned and is intended to be used in particular in stochastic metaheuristics. The MIDACO software is available in several programming languages, including MATLAB [31].

Developed by Yang and Deb [32, 33], Cuckoo Search (CS) is an optimization algorithm inspired by the behaviour of the cuckoo bird in searching for its eggs, which it incubates in the nests of other birds. The Firefly Algorithm (FA) proposed by Yang [34] is a metaheuristic algorithm inspired by the flashing patterns of tropical fireflies. Simulated Annealing (SA), introduced by Kirk-Patrick et al [35], is based on the idea of annealing in metallurgy, where metals are cooled and heated to change their physical properties. The functions of the last three algorithms developed in MATLAB by Yang [33], freely available from the MATLAB Central File Exchange [36-38], have been adapted for optimization.

Originally invented by Geem et al. [39], the Harmony Search (HS) algorithm is a metaheuristic optimizer inspired by the phenomenon that musicians repeatedly adjust the pitch of each instrument to eventually reach a beautiful state of harmony. The free MATLAB code for optimization with constraints available from MATLAB Central File Exchange [40] was used for the computations. The MATLAB programs CS, FA, SA, and HS used for the optimization in this paper are simple versions of metaheuristic algorithms with ordinary static penalty functions. All 5 MATLAB programs were modified to include custom objective and constraint functions.

For comparison, the Quasi-Monte Carlo (QMC) method [41] was also used to find optimal solutions for a linear BFD. An algorithm of the program developed in MATLAB is described in the paper by Kaminski [42]. This program uses an open-access MATLAB function developed by Burkhardt [43] to generate quasi-random numbers based on Hammersley's points [44]. Unlike metaheuristic algorithms, the QMC algorithm rigorously checks the fulfilment of inequality constraints.

The optimal values of the BFD coefficients were calculated by the process of minimizing the following objective function:

$$OF = \frac{w_1[\sum(f_1-z)^2+(f_2-z)^2]+w_2\sum(f_{21}-f_{22})^2}{w_1+w_2} \tag{13}$$

where: w_i – weighting factor, z – braking rate.

OF calculations were carried out for braking rate from 0.1 to 0.66 with a step of 0.01. The values of the weighting coefficients w_1=0.6 and w_2=(1-w_1)=0.4 were taken arbitrarily. Due to the stochastic nature of metaheuristic algorithms, the calculation was repeated 3 times, taking the final result with the lowest OF value.

To determine the adhesion utilization rates for each axle/axle combination (f_i, f_{2i}) occurring in the OF function, it is required to calculate the vertical axle load during braking as a function of the trailer braking rate, as described in the following sections. In the adopted rigid two-dimensional model of trailers, aerodynamic drag, and rolling resistance were omitted for simplicity. It was presumed that the deceleration-inducing brake forces T_i and/or T_{2i} are known functions of the brake pressure [45]. Changes to some suspension dimensions for different load statuses have also been omitted.

OPTIMISING BRAKING DISTRIBUTION ON TWO-AXLE TRAILERS

The two-axle chassis is used for trailers with a permissible weight of up to 18 tonnes [46]. Using the notation in Figure 2, the equations for the balance of forces and moments acting on the braking trailer are of the following form:

$$\sum X = z \cdot G - T_1 - T_2 = 0 \tag{14}$$

$$\sum Z = R_1 + R_1 - G = 0 \tag{15}$$

$$\sum M_1 = R_2 L_1 - G \cdot a + z \cdot G \cdot h = 0 \tag{16}$$

where: T_1, T_2 – front and rear axle braking forces, R_1, R_2 – axle loads, L_1 – inter-axle spacing, a – distance from gravity centre (GC) to the front axle, h – GC height, G – trailer weight, z – braking rate.

Based on the equations above, it is possible to calculate the load on the axles as a function of the braking rate z:

$$R_1 = \frac{G}{L_1}(b + h \cdot z) \qquad R_2 = \frac{G}{L_1}(a - h \cdot z) \tag{17}$$

where: b – horizontal distance between GC and rear axle, $b=L_1-a$.

For a two-axle trailer, the limits of the directional coefficient i_P of the BFD line crossing through the origin of the coordinate system T_2=f(T_1) can be determined from the permissible ranges of the relative brake forces of front γ_1 and rear γ_2 axles:

$$\gamma_1 = \frac{T_1}{G} = \frac{R_1 f_1}{G} = \left(\frac{b}{L} + \frac{h}{L}z\right) f_1 \qquad \gamma_2 = \frac{T_2}{G} = \frac{R_2 f_2}{G} = \left(1 - \frac{b}{L} - \frac{h}{L}z\right) f_2 \tag{18}$$

By substituting the limit values of adhesion utilization f_1, f_2 for a given trailer in relation (18), it is possible to determine the corresponding permissible area of relative braking forces on the graph γ_2=f(γ_1). The results of the calculations for unladen and laden trailers are shown in Figures 3 and 4 respectively.

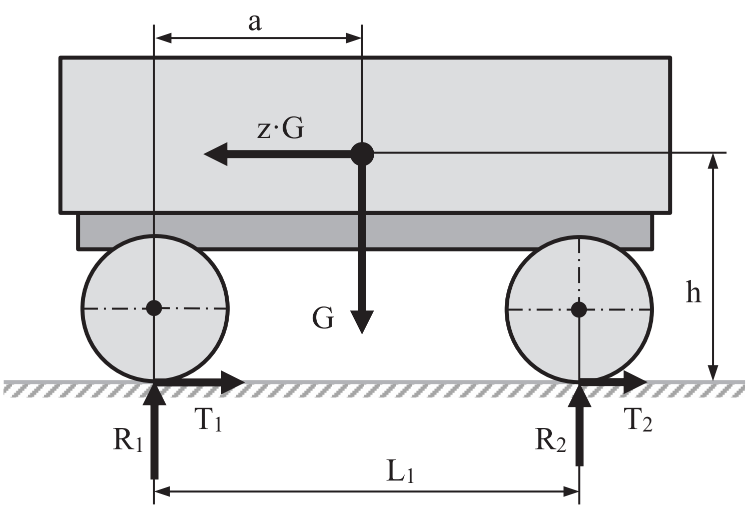

Figure 2. Forces acting on the two-axle braking trailer (according to ISO coordinate system [47])

The first solution is represented by the AB and CD lines in Figure 3-a, Figure 4-a for the adhesion utilization rates, and the corresponding curves in Figure 3-b and Figure 4-b for the brake force limits in the coordinate system γ_1-γ_2. In the second solution, the limits of the admissible range of f_1, and f_2 rates are represented by the lines MN and JKL in Figures 3-c and 4-c. The related ranges of relative braking forces γ_1, and γ_2 are shown in Figure 3-d and Figure 4-d for an unladen and laden trailer respectively. The formulae for the border lines and curves in the $f_{1,2}$-z and γ_1-γ_2 system, along with the coordinates of each point, are listed in Table 1 and Table 2.

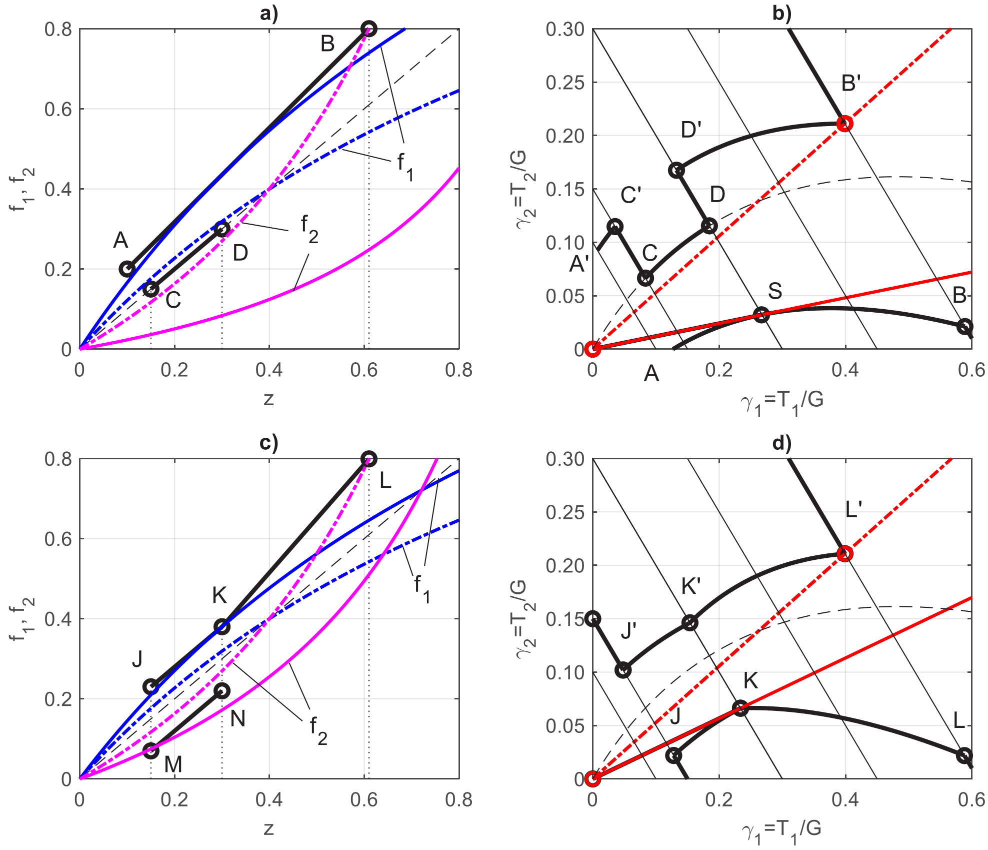

Figure 3. Linear BFD for unladen two-axle trailer of 4200 kg: a, c - runs f_1, f_2 of the adhesion utilization of the axles; b - limits of the distribution coefficient for solution 1; d - limits of the distribution coefficient for solution 2; a = 1.48 m, L = 2.95 m, h = 1.15 m

Table 1. BFD curve formulae for two-axle trailers

Curve	Coordinate system z-$f_{1,2}$	Coordinate system γ_1-γ_2	Range
A-B	$f_{1,2} \le \frac{(z+0.07)}{0.85}$	$\gamma_1 = \left(\frac{b}{L} + \frac{h}{L}z\right)\left(\frac{z+0.07}{0.85}\right)$	z=0.1-0.61
C-D	$f_1 > z > f_2$	$\gamma_1 = \left(\frac{b}{L} + \frac{h}{L}z\right)z$	z=0.15-0.30
A'-C' D'-B'	$f_{1,2} \le \frac{(z+0.07)}{0.85}$	$\gamma_1 = z - \left(\frac{a}{L} - \frac{h}{L}z\right)\left(\frac{z+0.07}{0.85}\right)$	z=0.1-0,15 z=0.3-0.61
J-K	$f_{1,2} \le z + 0.08$	$\gamma_1 = max\left(\left(\frac{b}{L} + \frac{h}{L}z\right)(z+0.08);\ z\left(\frac{a}{L} - \frac{h}{L}z\right)(z-0.08)\right)$	z=0.15-0.30
M-N	$f_1 \ge z - 0.08$	$\gamma_1 = max\left(\left(\frac{b}{L} + \frac{h}{L}z\right)(z-0.08);\ z - \left(\frac{a}{L} - \frac{h}{L}z\right)(z+0.08)\right)$	z=0.15-0.30
K-L	$f_{1,2} \le \frac{(z-0.02)}{0.74}$	$\gamma_1 = \left(\frac{b}{L} + \frac{h}{L}z\right)\left(\frac{z-0.3}{0.74} + 0.38\right)$	z=0.30-0.61
K'-L'	$f_{1,2} \le \frac{(z-0.02)}{0.74}$	$\gamma_1 = z - \left(\frac{a}{L} - \frac{h}{L}z\right)\left(\frac{z-0.3}{0.74} + 0.38\right)$	z=0.30-0.61

Table 2. Coordinates of characteristic points (for all ranges $\gamma_2 = z - \gamma_1$)

Point	z	$f_{1,2}$	γ_1
A	0.10	0.20	$0.2\left(\frac{b}{L} + 0.1 \cdot \frac{h}{L}\right)$
B	0.61	0.80	$0.8\left(\frac{b}{L} + 0.61 \cdot \frac{h}{L}\right)$
C	0.15	0.15	$0.15\left(\frac{b}{L} + 0.15 \cdot \frac{h}{L}\right)$
D	0.30	0.30	$0.3\left(\frac{b}{L} + 0.3 \cdot \frac{h}{L}\right)$
A'	0.10	0.20	$0.1 - 0.2\left(\frac{a}{L} - 0.1 \cdot \frac{h}{L}\right)$
C'	0.15	0.259	$0.15 - \left(\frac{0.22}{0.85}\right)\left(\frac{a}{L} - 0.15 \cdot \frac{h}{L}\right)$
D'	0.30	0.435	$0.3 - \left(\frac{0.37}{0.85}\right)\left(\frac{a}{L} - 0.3 \cdot \frac{h}{L}\right)$
B'	0.61	0.8	$0.61 - \left(\frac{0.68}{0.85}\right)\left(\frac{a}{L} - 0.61 \cdot \frac{h}{L}\right)$
J	0.15	0.23	$min\left(0.23\left(\frac{b}{L} + 0.15 \cdot \frac{h}{L}\right);\ 0.15 - 0.07\left(\frac{a}{L} - 0.15 \cdot \frac{h}{L}\right)\right)$
K	0.30	0.38	$max\left(0.38\left(\frac{b}{L} + 0.3 \cdot \frac{h}{L}\right);\ 0.3 - 0.22\left(\frac{a}{L} - 0.3 \cdot \frac{h}{L}\right)\right)$
L	0.61	0.8	$\left(\frac{b}{L} + 0.61 \cdot \frac{h}{L}\right)\left(\frac{0.31}{0.74} + 0.38\right)$
M	0.15	0.07	$max\left(0.07\left(\frac{b}{L} + 0.15 \cdot \frac{h}{L}\right);\ 0.15 - 0.23\left(\frac{a}{L} - 0.15 \cdot \frac{h}{L}\right)\right)$
N	0.30	0.22	$min\left(0.22\left(\frac{b}{L} + 0.3 \cdot \frac{h}{L}\right);\ 0.3 - 0.38\left(\frac{a}{L} - 0.3 \cdot \frac{h}{L}\right)\right)$
K'	0.30	0.38	$0.38\left(\frac{a}{L} - 0.3 \cdot \frac{h}{L}\right)$
L'	0.61	0.8	$0.61 - \left(\frac{a}{L} - 0.61 \cdot \frac{h}{L}\right)\left(\frac{0.31}{0.74} + 0.38\right)$

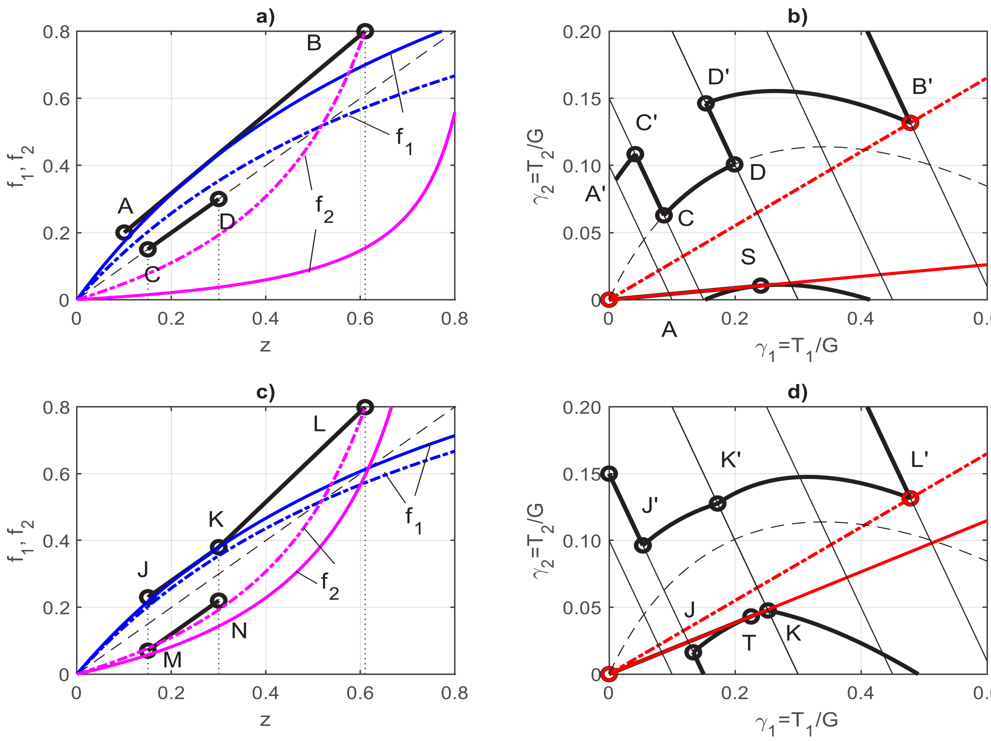

Figure 4. Linear BFD for a laden two-axle trailer of 16250 kg: a, c - runs f_1, f_2 of the adhesion utilization of the axles; b - limits of the distribution coefficient for solution 1; d - limits of the distribution coefficient for solution 2; a = 1.48 m, L = 2.95 m, h = 1.63 m

From the graphs γ_2=f(γ_1)it is possible to determine the permissible values of the directional coefficient $i_p=\gamma_2/\gamma_1$ of the linear distribution of the braking forces. For a given point P:

$$i_P=\frac{\gamma_{2p}}{\gamma_{1p}}=\frac{\left(\frac{a}{L}-z_p\cdot\frac{h}{L}\right)f_2}{\left(\frac{b}{L}+z_p\cdot\frac{h}{L}\right)f_1} \tag{19}$$

For the first solution, the area of acceptable BFD is bounded at the top by a line passing through point D or B' (select the line with the lower direction coefficient) and at the bottom by the OS line tangent to the AB boundary curve at point S (Figures 3-b and 4-b).

$$z_S=0.1\sqrt{7\frac{b}{h}}\quad \gamma_{1S}=\left(\frac{b}{L}+\frac{h}{L}z_S\right)\left(\frac{z_S+0.07}{0.85}\right)\quad \gamma_{2S}=z_S-\gamma_{1S} \tag{20}$$

For the second solution, the linear BFD upper bound is a straight line through point L' (Figures 3-d and 4-d). From below, the allowable area is bounded by a straight line tangent to the JK curve at point T (Figure 4-d):

$$z_T=min\begin{cases}0.2\sqrt{2\frac{b}{h}}\\0.2\sqrt{2\frac{a}{h}}\end{cases}\quad \gamma_{1T}=max\begin{cases}\left(\frac{b}{L}+\frac{h}{L}z_T\right)(z_T+0.08)\\z_T-\left(\frac{a}{L}-\frac{h}{L}z_T\right)(z_T-0.08)\end{cases}\quad \gamma_{2T}=z_T-\gamma_{1T} \tag{21}$$

If the tangent point T is out of the JK section of the boundary curve, the direction coefficient of the lower boundary line is calculated from the point K coordinates (Figure 4-d). The limit values of the directional coefficients i_P and the corresponding brake force distribution coefficients β_1 for the two-axle trailer considered, as well as the optimum values of β_1 obtained using the different MOAs, are summarised in Table 3.

Table 3. Limiting and optimum β_1 ratios for linear BFD for two-axle trailer

The first solution acc. to (3), (4)		
Limits	$i_{min}=i_S=0.1202$, $\beta_{1max}=0.8927$	$i_{min}=i_S=0.0434$, $\beta_{1max}=0.9584$
	$i_{max}=i_{B'}=0.5293$, $\beta_{1min}=0.6539$	$i_{max}=i_{B'}=0.2754$, $\beta_{1min}=0.7841$
Algorithm	Unladen trailer	Laden trailer
QMC	β_1=0.6913, OF=0.07653	β_1=0.7841, OF=0.2408
MIDACO, CS, FA, HS	β_1=0.6913, OF=0.07653	β_1=0.7828, OF=0.2406
SA	β_1=0.6912, OF=0.07653	β_1=0.7828, OF=0.2406
The second solution acc. to (5), (6)		
Limits	$i_{min}=i_K=0.2832$, $\beta_{1max}=0.7793$	$i_{min}=i_T=0.1914$, $\beta_{1max}=0.8393$
	$i_{max}=i_{L'}=0.5293$, $\beta_{1min}=0.6539$	$i_{max}=i_{L'}=0.2754$, $\beta_{1min}=0.7841$
Algorithm	Unladen trailer	Laden trailer
QMC	β_1=0.6913, OF=0.07653	β_1=0.7841, OF=0.2408
MIDACO, CS, FA, HS	β_1=0.6913, OF=0.07653	β_1=0.7828, OF=0.2406
SA	β_1=0.6914, OF=0.07653	β_1=0.7829, OF=0.2406

For the unladen trailer, the optimum β_1 values calculated using the QMC method and the heuristic methods are almost the same. There are slight differences in the results, obtained using the SA method, but the differences do not exceed 0.03%. For the laden trailer, identical results were obtained using heuristic methods for both the first and second solutions. Examples of adhesion utilization curves $f_i(z)$ are shown in Figure 5. However, it should be noted that the optimum value β_1 obtained by heuristic methods for a laden trailer is less than the permissible limit β_{1min} (according to MIDACO $k_p=(1-\beta_1)/\beta_1=0.2774$) and the curve f_2 exceeds the permissible zone (Figure 6). It is worth noting that heuristic methods are not strictly accurate methods, especially in the case of optimization with constraints using a penalty function. In the case of the QMC method, the optimal value of β_1 is equal to the constraint β_{1min}=0.7841 for both solutions.

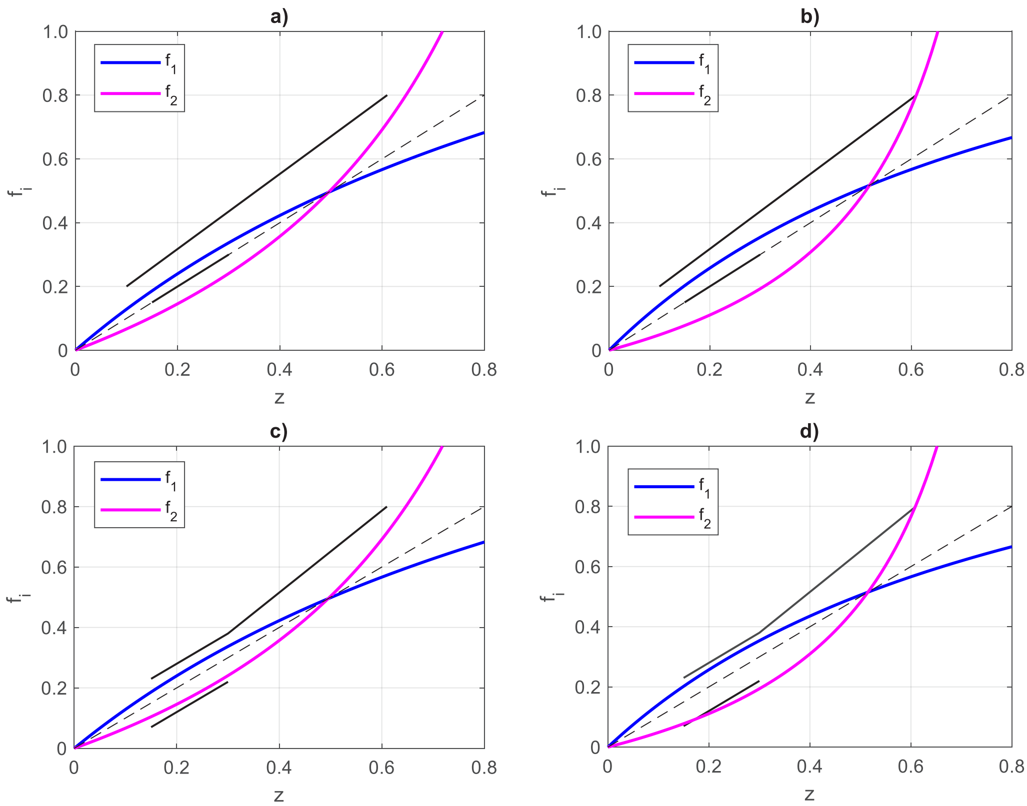

Figure 5. Utilized adhesion curves $f_i(z)$ for optimum BFD in two-axle trailer: a - unladen trailer, QMC method, I solution, b - laden trailer, QMC method, I solution, c - unladen trailer, MIDACO method, II solution, d - laden trailer MIDACO method, II solution

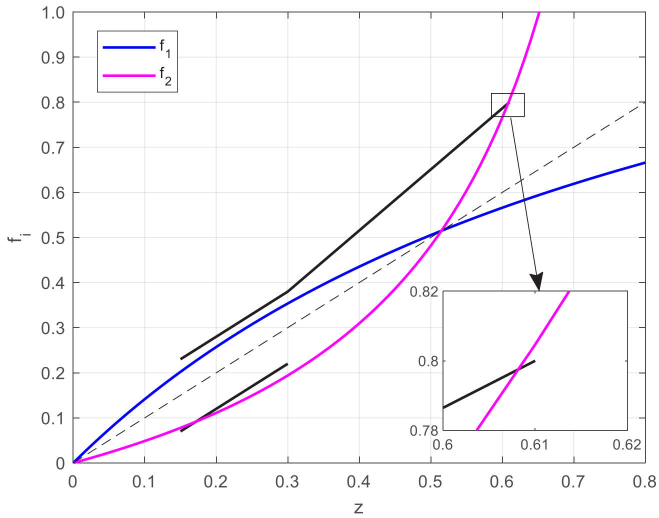

Figure 6. Utilized adhesion curves $f_i(z)$ for optimum BFD in a laden two-axle trailer (MIDACO, II solution)

OPTIMISING BRAKING DISTRIBUTION ON THREE-AXLE TRAILERS

Heavy farm trailers of around 25 tonnes GVW can be fitted with a three-axle chassis [46]. These are usually connected to the tractor by a single-point drawbar, which is used to steer the front axle, and tandem axles are fitted to the rear of the trailer. Tandem units are used to increase payload and distribute it between both axles regardless of road unevenness [16].

The dynamic model of the three-axle trailer during braking is shown in Figure 7. Thus defined, the braked trailer model is compatible with any tandem suspension model.

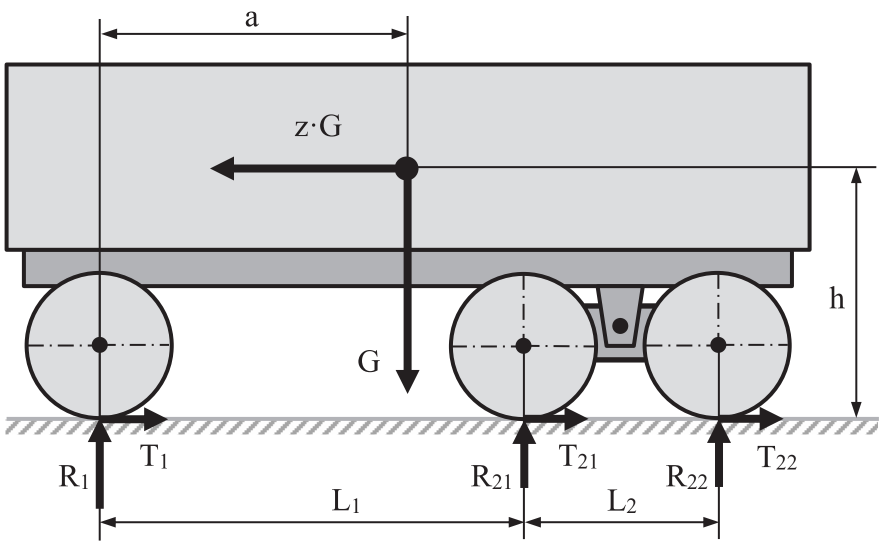

Figure 7. Forces acting on three-axle trailer with tandem suspension: L_1=4.35 m, L_2=1.35 m, m=7700/24000 kg, a=3.11/3.04 m, h=1.19/1.57 m

Using the notation from Figure 7, the force and moment equilibria are written as:

$$\sum X = z \cdot G - T_1 - T_{21} - T_{22} = 0 \tag{22}$$
$$\sum Z = R_1 + R_{21} + R_{22} - G = 0 \tag{23}$$
$$\sum M_1 = R_{21}L_1 + R_{22}(L_1 + L_2) - G \cdot a + z \cdot G \cdot h = 0 \tag{24}$$

where: G – trailer weight, T_1, T_{21}, T_{22} – braking forces, R_1, R_{21}, R_{22} – loads, L_1 – inter-axle spacing, L_2 – tandem axle spread, a – distance from GC to the front axle, h – GC height.

For the determination of all vertical forces, the system of equations (22)-(24) must be completed by an additional equation between reactions R_{21} and R_{22}, which requires an analysis of the forces acting on the specific tandem suspension.

Bogie suspension

One of the simple forms of a tandem unit is a mechanical bogie suspension [48], [49]. The bogie suspension is designed to adapt to different types of terrain and road conditions, making it a versatile option for agricultural trailers that need to operate in different environments. Axles equipped with ABS can be used at a speed of up to 65 km/h [48]. In the bogie suspension, parabolic tapered springs are attached upside down to the trailer frame (Fig. 8) using a cradle and U-bolts to allow movement between the axles [49].

Considering the forces and moments applied to the bogie axles (Fig. 8), the following system of equilibrium equations is obtained:

$$\sum X = z \cdot G_2 - T_{21} - T_{22} + T_2 = 0 \tag{25}$$
$$\sum Z = R_{21} + R_{22} - R_2 - G_2 = 0 \tag{26}$$
$$\sum M_2 = R_{22}d_2 - R_{21}d_1 + G_2b_2 - z \cdot G_2(h_s - h_2) + (T_{21} + T_{22})h_s = 0 \tag{27}$$

where: T_2, R_2 - horizontal and vertical reactions in the suspension support, d_1, d_2 - parabolic spring lengths, h_s - height of support position, b_2 - distance from a support to the centre of unsprung weight G_2, h_2 - height of the centre of G_2.

By solving equations (23), (24) and (27) together, taking into account from equation (22) that $T_{21} + T_{22} = z \cdot G - T_1$, the vertical axle loads are given by:

$$R_1 = G\left(1 - \frac{a}{L} + z\frac{h}{L}\right) - G_2\left(\frac{b_2}{L} - z\frac{h_s-h_2}{L}\right) - (z \cdot G - T_1)\frac{h_s}{L} \tag{28}$$
$$R_{21} = G\left(\frac{a}{L} - z\frac{h}{L}\right)\frac{d_2}{L_2} + \frac{L_1+L_2}{L_2}\left[G_2\left(\frac{b_2}{L} - z\frac{h_s-h_2}{L}\right) + (z \cdot G - T_1)\frac{h_s}{L}\right] \tag{29}$$
$$R_{22} = G\left(\frac{a}{L} - z\frac{h}{L}\right)\frac{d_1}{L_2} - \frac{L_1}{L_2}\left[G_2\left(\frac{b_2}{L} - z\frac{h_s-h_2}{L}\right) + (z \cdot G - T_1)\frac{h_s}{L}\right] \tag{30}$$

where: $L_2 = d_1 + d_2$ - tandem wheelbase, $L = L_1 + d_1$ - trailer wheelbase.

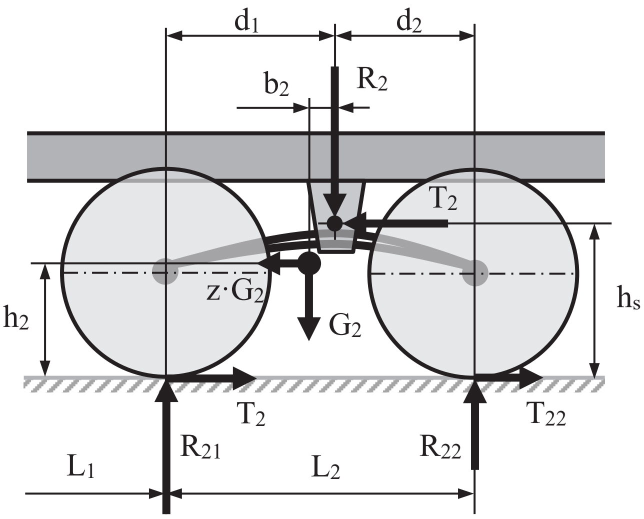

Figure 8. Forces acting on a bogie suspension: d_1=0.705 m, d_2=0.645 m, h_s=0.567 m, h_2=0.547 m, b_2=0.03 m

Optimal values of BFD ratios β_1 for the three-axle trailer with bogie suspension obtained by various simulation methods are summarized in Table 4.

Table 4. Optimal values of ratios β_1, and β_{21}, for a linear BFD for a three-axle trailer with bogie suspension

The first solution acc. to (3), (4)		
Algorithm	Unladen trailer	Laden trailer
QMC	β_1=0.5059, β_{21}=0.3319, OF=0.15449	β_1=0.5569, β_{21}=0.2998, OF=0.17836
MIDACO, CS	β_1=0.5089, β_{21}=0.3287, OF=0.15429	β_1=0.5609, β_{21}=0.2951, OF=0.17764
FA	β_1=0.5090, β_{21}=0.3286, OF=0.15429	β_1=0.5608, β_{21}=0.2952, OF=0.17764
SA	β_1=0.5080, β_{21}=0.3295, OF=0.15430	β_1=0.5615, β_{21}=0.2947, OF=0.17765
HS	β_1=0.5089, β_{21}=0.3288, OF=0.15429	β_1=0.5609, β_{21}=0.2951, OF=0.17764
The second solution acc. to (5), (6)		
Algorithm	Unladen trailer	Laden trailer
QMC	β_1=0.5059, β_{21}=0.3319, OF=0.15449	β_1=0.5569, β_{21}=0.2998, OF=0.17836
MIDACO, CS	β_1=0.5089, β_{21}=0.3287, OF=0.15429	β_1=0.5609, β_{21}=0.2951, OF=0.17764
FA	β_1=0.5088, β_{21}=0.3288, OF=0.15429	β_1=0.5607, β_{21}=0.2953, OF=0.17764
SA	β_1=0.5083, β_{21}=0.3294, OF=0.15429	β_1=0.5609, β_{21}=0.2952, OF=0.17764
HS	β_1=0.5088, β_{21}=0.3288, OF=0.15429	β_1=0.5609, β_{21}=0.2951, OF=0.17764

The results of the BFD coefficients for solutions I and II for the boogie tandem suspension are almost identical (Fig. 9). The share of each axle in the total brake force is approximately β_1=50.9%, β_{21}=32.9% and β_{22}=16.2% for the unladen trailer and β_1=56.1%, β_{21}=29.5% and β_{22}=14.4% for the laden trailer. The results fully meet the requirements of Regulation UE 2015/68. They exhibit a superior fit to the ideal distribution obtained using metaheuristic algorithms, with a marginally lower value of the OF than when using the QMC method.

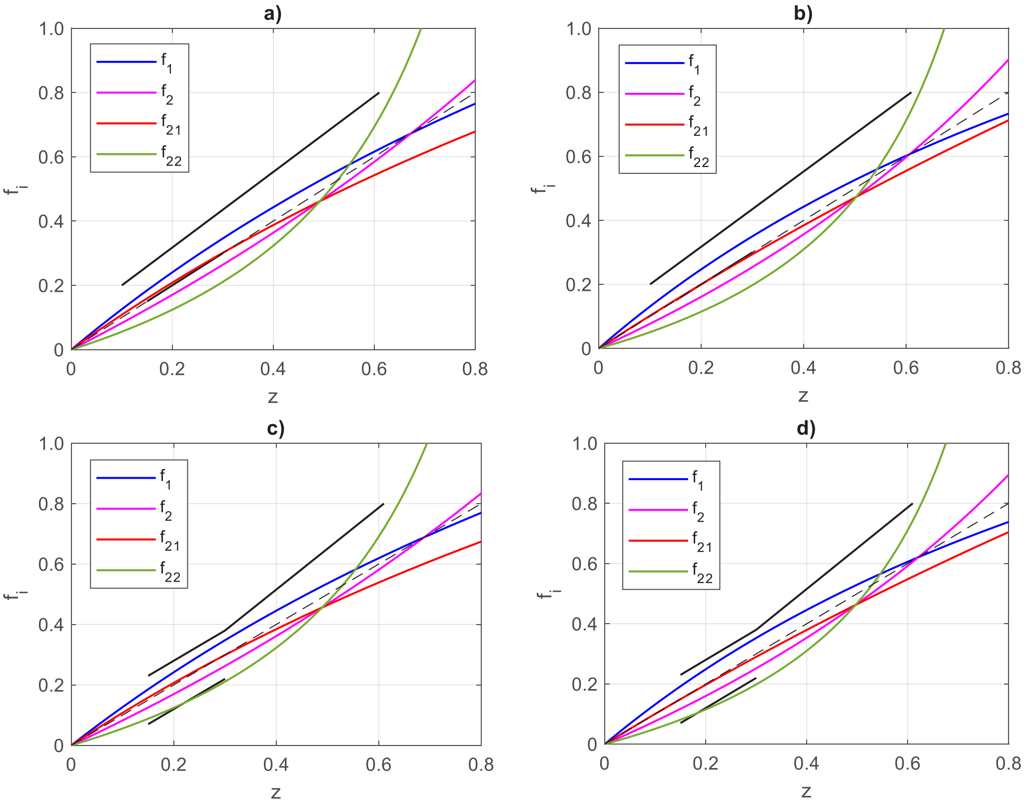

Figure 9. Utilized adhesion curves $f_i(z)$ for optimal BFD in three-axle trailer: a - an unladen trailer, QMC method, I solution, b - a laden trailer, QMC method, I solution, c - an unladen trailer, CS method, II solution, d - a laden trailer CS method, II solution

Two-leaf spring suspension

Another common mechanical tandem suspension used on agricultural trailers is two-leaf spring suspension, most often with slipper springs [48], [49]. Slipper spring has a single eye at one end and a flat, tapered end at the other. The front eye of the spring is hinged to the front hanger (leading axle) and the levelling beam (trailing axle). The rear end of the spring is attached to the levelling beam (Figure 10).

For a leading axle with an unsprung weight of G_{21}, the equations of forces and moments are as follows:

$$\sum X = z \cdot G_{21} - T_{21} + T_3 = 0 \tag{31}$$

$$\sum Z = R_{21} - R_3 - R_{32} - G_{21} = 0 \tag{32}$$

$$\sum M_3 = -R_{32}c + R_{21}c_1 - G_{21}c_1 - z \cdot G_{21}(h_s - h_2) + T_{21}h_s = 0 \tag{33}$$

For a trailing axle with an unsprung weight of G22, these equations take the form:

$$\sum X = z \cdot G_{22} - T_{22} + T_4 = 0 \tag{34}$$

$$\sum Z = R_{22} - R_4 - R_{42} - G_{22} = 0 \tag{35}$$

$$\sum M_4 = R_{42}c - R_{22}c_2 + G_{22}c_2 - z \cdot G_{22}(h_s - h_2) + T_{22}h_s = 0 \tag{36}$$

Calculated from equations (33) and (36), the forces acting on the ends of the levelling beam are of the form:

$$R_{32} = (R_{21} - G_{21})\frac{c_1}{c} - z \cdot G_{21}\frac{h_s - h_2}{c} + T_{21}\frac{h_s}{c} \tag{37}$$

$$R_{42} = (R_{22} - G_{22})\frac{c_2}{c} + z \cdot G_{22}\frac{h_s - h_2}{c} - T_{22}\frac{h_s}{c} \tag{38}$$

The forces R_{32} and R_{42} are related by the equation of moments acting on the levelling beam:

$$R_{32}d_1 = R_{42}d_2 \tag{39}$$

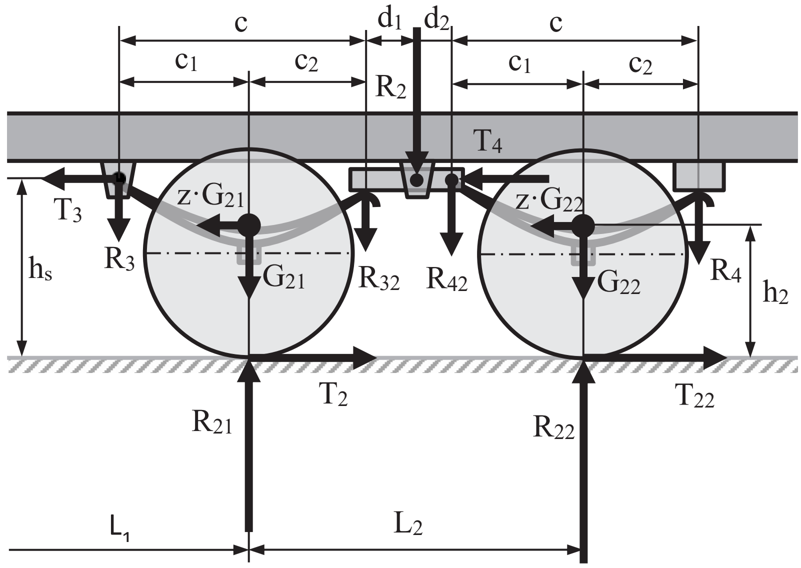

Figure 10. Forces acting on a two leaf spring suspension: d_1=d_2=0.21 m, h_s=0.717 m, h_2=0.567 m, c_1=0.454 m, c=0.93 m

Substituting (37) and (38) into (39) gives the relationship between the reactions R_{21} and R_{22} which, together with equations (23) and (24), can be used to determine the axle loads when braking the trailer:

$$R_1 = G - \frac{L_2}{MN}\Big\{G(a - z \cdot h)\frac{c_1(d_1 - d_2) + c \cdot d_2}{L_2} + G_{21}d_1[c_1 + z(h_s - h_2)] - G_{22}d_2[c_2 - z(h_s - h_2)] - (T_{21}d_1 + T_{22}d_2)h_s\Big\} \quad (40)$$

$$R_{21} = \frac{L_1 + L_2}{MN}\Big\{G(a - z \cdot h)\frac{d_2 c_2}{L_1 + L_2} + G_{21}d_1[c_1 + z(h_s - h_2)] - G_{22}d_2[c_2 - z(h_s - h_2)] - (T_{21}d_1 + T_{22}d_2)h_s\Big\} \quad (41)$$

$$R_{22} = \frac{L_1}{MN}\Big\{G(a - z \cdot h)\frac{c_1 d_1}{L_1} - G_{21}d_1[c_1 + z(h_s - h_2)] + G_{22}d_2[c_2 - z(h_s - h_2)] + (T_{21}d_1 + T_{22}d_2)h_s\Big\} \quad (42)$$

where: $MN = c_2 d_2 L_1 + c_1 d_1 (L_1 + L_2)$

The results of optimizing the BFD for a trailer with two-leaf spring suspension are summarised in Table 5.

Table 5. Optimal values of ratios β_1, β_{21}, for a linear BFD for a three-axle trailer with two leaf spring suspension

The first solution acc. to (3), (4)		
Algorithm	Unladen trailer	Laden trailer
QMC	β_1=0.6620, β_{21}=0.0730, OF=0.56170	β_1=0.7020, β_{21}=0.0623, OF=0.63207
MIDACO, CS, HS	β_1=0.6654, β_{21}=0.0734, OF=0.56117	β_1=0.7018, β_{21}=0.0636, OF=0.63099
FA	β_1=0.6654, β_{21}=0.0734, OF=0.56117	β_1=0.7019, β_{21}=0.0636, OF=0.63099
SA	β_1=0.6655, β_{21}=0.0739, OF=0.56128	β_1=0.7022, β_{21}=0.0634, OF=0.63105
The second solution acc. to (5), (6)		
Algorithm	Unladen trailer	Laden trailer
QMC	β_1=0.6009, β_{21}=0.0371, OF=1.11104	β_1=0.6426, β_{21}=0.0267, OF=1.36936
MIDACO	β_1=0.6143, β_{21}=0.0584, OF=0.73816	β_1=0.6546, β_{21}=0.0474, OF=0.87157
CS	β_1=0.6143, β_{21}=0.0584, OF=0.73832	β_1=0.6544, β_{21}=0.0474, OF=0.87183
FA	β_1=0.6142, β_{21}=0.0578, OF=0.73898	β_1=0.6544, β_{21}=0.0476, OF=0.87192
SA	β_1=0.6141, β_{21}=0.0582, OF=0.74012	β_1=0.6543, β_{21}=0.0470, OF=0.87211
HS	β_1=0.6143, β_{21}=0.0584, OF=0.73833	β_1=0.6544, β_{21}=0.0473, OF=0.87183

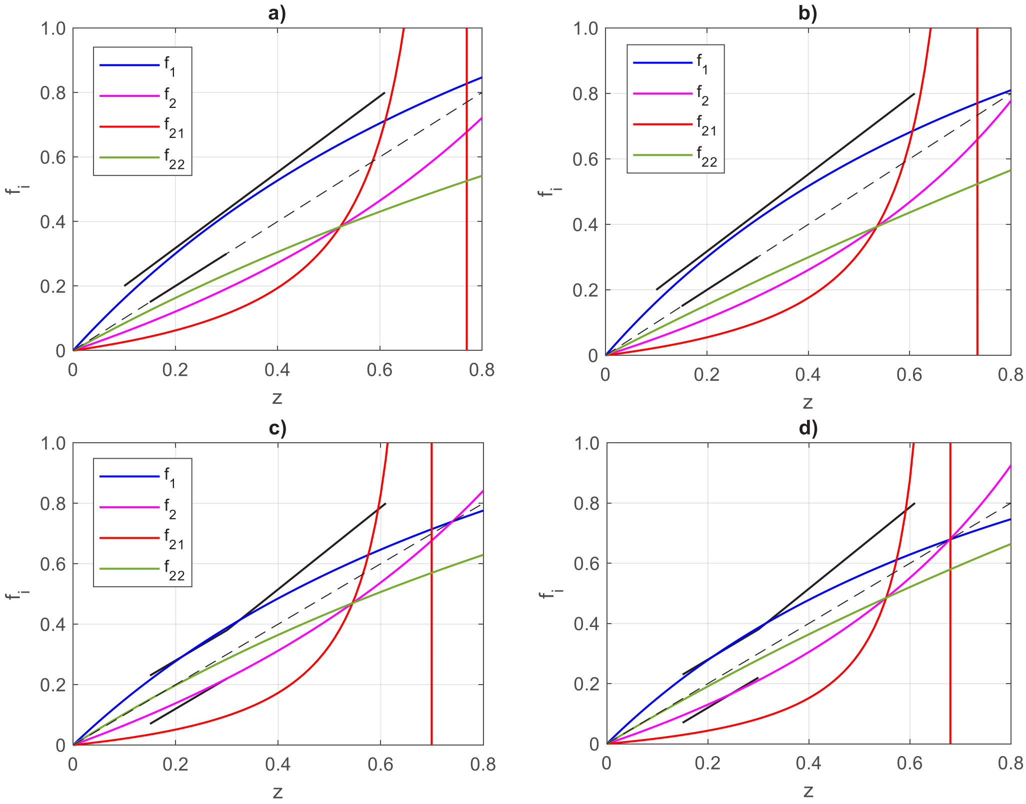

Figure 11. Utilized adhesion curves $f_i(z)$ for an optimal BFD in a three-axle trailer: a - unladen trailer, QMC method, I solution, b - laden trailer, QMC method, I solution, c - unladen trailer, FA method, II solution, d - laden trailer FA method, II solution

The two-leaf spring suspension yielded similar optimum braking force distribution coefficients for the first solution only. The share of each axle in the total braking force is approximately β_1=66.5%, β_{21}=7.3%, and β_{22}=26.2% for the empty trailer and β_1=70%, β_{21}=6.4% and β_{22}=23.6% for the loaded trailer. The objective function values obtained using the metaheuristic algorithms were consistently smaller than those obtained using the QMC method.

The results obtained by the metaheuristic methods and the QMC method for solution II show significant discrepancies. The average values of the BFD coefficients for the metaheuristic methods are as follows: β_1=61.4%, β_{21}=5.8%, and β_{22}=32.8% for the unladen trailer, and β_1=65.5%, β_{21}=4.7%, and β_{22}=29.8% for the laden trailer. Solution II shows that the objective function values obtained by the metaheuristic methods are significantly smaller than those obtained by the QMC method. It must be emphasized, however, that for such a BFD, the waveforms of the f_{21} curve of adhesion utilized by the leading tandem axle fall outside the permissible area when achieving a value of z=0.6, as shown in Figure 11-c,d. Furthermore, the data clearly show that for both solutions I and II, the dynamic load on the leading axle reaches zero at a braking rate of about 0.7, which means that the wheels of this axle detach from the ground. Figure 11 clearly shows that for z≈0.7 the f_{21} curve approaches infinity and then drops below zero (calculations for f_{21}<0 are not physically meaningful). This is a direct result of the significant variation in brake forces of tandem axles with this suspension. The rear axle is slightly under-braked and the front axle is heavily under-braked, as confirmed in the literature [16, 17]. This phenomenon is dangerous because braking with very low vertical loads can cause wheel lockup on the leading tandem axle. From the optimum ratios β_1, and β_{21} summarised in Tables 4 and 5, it can be seen that the BFD of a three-axle trailer depends significantly on the load status and the tandem unit used on the trailer.

APPLICATION MECHANISM DESIGN

Based on the BFD determined for a laden trailer, the required braking forces and torques for each axle can be calculated for a braking rate of z=0.5, achieved at a pressure of p=6.5 bar for air and p=115 bar for hydraulic braking systems. On this basis, the braked axles are selected from the catalogue, and the basic parameters of the application mechanism are determined, including the number and size of the actuators (stroke and effective area) and the length of the slack adjuster.

The brake actuator force is calculated from the manufacturer's data using the following generalized relationship:

$$F_a = A \cdot p - B \tag{43}$$

where: p – pressure in actuation system, A, B – coefficients.
The camshaft input torque is the product of the brake actuator force F_a and the slack adjuster length l:

$$C = F_a l \tag{44}$$

The axle manufacturer's formulae are used to calculate the brake force of the i-th axle [1], [45]:

$$T_i = k \cdot (C - C_0) \cdot \eta \cdot \frac{BF}{r_d} \tag{45}$$

where: k – number of brake actuators, C_0 – threshold camshaft input torque, η – mechanical efficiency, r_d - rolling wheel radius, BF – brake factor described by the relation [45]:

$$BF = \frac{C^* \cdot r_e}{2r_b} \tag{46}$$

where: C^* - braking efficiency factor, r_e – effective radius of friction, r_b - effective cam radius.

CONCLUSIONS

The values of the optimum BFD coefficients obtained by the metaheuristic methods are very close to those obtained by the QMC method. However, the analysis of the results shows that in some cases the adhesion curves utilized by the axles do not fully comply with the requirements of Directive 68/2015, despite lower OF values compared to the QMC method. The requirements, which are essentially inequality constraints, have been incorporated into the metaheuristic algorithms in the form of a penalty function. The penalty-based method transforms constrained optimization into unconstrained one by adding a penalty to the original OF. The disadvantage of this method is that the solution to the problem without constraints will not be an accurate solution to the original problem, because the margin of violation of the constraints is allowed as long as a significant improvement of the OF is obtained. The QMC algorithm, on the other hand, treats constraints strictly. Failure to satisfy any of these results in successive draws of the decision variables.

However, as already mentioned, the differences observed between the BFD optimization results obtained by the MOM and QMC methods are small and acceptable, especially in the early stages of brake system design. It should be pointed out that the selection of the brake axle parameters (brake mechanism, actuators) is iterative, since some parameters, such as brake lever length and actuator area and stroke, have discrete values.

The advantage of metaheuristic methods is the free availability of open-source software developed in various programming environments such as MATLAB, Scilab, Octave, C, C++, and others, which only require the user to edit his own objective and penalty functions. The use of optimization methods, especially metaheuristics, is particularly useful for three-axle trailers where the BFD is influenced by the tandem suspension parameters. Metaheuristic methods can also be recommended for the selection of BFD for two-axle trailers. These are less labour-intensive than analytical methods which require the calculation of characteristic point coordinates and curve equations in the γ_1-γ_2 system.

From the obtained results of the metaheuristic optimization, the following conclusions can be drawn. For the two-axle trailer with a payload of approximately 12 tonnes, identical values for the coefficient β_1 of the linear BFD were obtained for almost all metaheuristic algorithms for both solution I and solution II. The largest deviations were observed for the SA algorithm. For the laden trailer, the rear axle adhesion curve f_2 slightly exceeds the permitted range.

Optimization calculations carried out using the MOMs and QMC method for the three-axle trailer with a payload of approximately 16 tonnes have revealed that the BFD is significantly dependent on the type of rear axle suspension. The lowest minimized OF values (around 0.154÷0.178) were obtained for bogie suspension. For both solutions, the contribution of each axle to the overall brake force is approximately β_1=50.9%, β_{21}=32.9%, and β_{22}=16.2% for the unladen trailer and β_1=56.1%, β_{21}=29.5%, and β_{22}=14.4% for the laden trailer. The results fully comply with the requirements of EU Regulation 2015/68.

Significantly higher values of the OF (around 0.665÷0.872) were obtained for two leaf spring tandem axles. In this case, the contribution of each axle to the total brake force is more variable and lies within the following limits: for β_1=61.5÷70%, for β_{21}=4.7÷7.3% and β_{22}=23.6÷32.8%, depending on the trailer load factor and the solution used. Furthermore, for a laden trailer, the leading axle adhesion curve f_{21} exceeds the higher limit of the permissible zone for z<0.61. Calculations have also shown that load transfer between tandem axles leads to premature wheel locking of the leading axle at a braking ratio of about 0.7.

Acknowledgements

This research was funded through a subsidy from the Ministry of Science and Higher Education of Poland, for the discipline of mechanical engineering at the Faculty of Mechanical Engineering at Bialystok University of Technology (WZ/WM-IIM/5/2023).

REFERENCES

1. Commission Delegated Regulation (EU) 2015/68 of 15 October 2014 supplementing Regulation (EU) No 167/2013 of the European Parliament and of the Council with regard to vehicle braking requirements for the approval of agricultural and forestry vehicles.
2. Glišović J., Lukić J., Šušteršič V., Ćatić D. 2015. Development of tractors and trailers in accordance with the requirements of legal regulations. In: Proc. of 9th International Quality Conference, Kragujevac, Serbia 2015, 193–202.
3. Caban A., Kidawski A., Włodarczyk A. Synchronization of the braking of heavy tractor-trailer and tractor-semitrailer units: operational problems. The Archives of Automotive Engineering – Archiwum Motoryzacji 2017; 77(3): 17-29. DOI: https://doi.org/10.14669/AM.VOL.77.ART2
4. Zhang N., Wu J., Li T., Zhao Z., Yin G. Influence of braking on dynamic stability of car-trailer combinations. Proceedings of the Institution of Mechanical Engineers, Part D: Journal of Automobile Engineering 2021; 235(2-3): 455-464. https://doi.org/10.1177/09544070209598
5. Mital A., Desai A., Subramanian A., Mital A. Product development: A structured approach to consumer product development, design, and manufacture. 2nd ed. Elsevier Science, 2014.
6. Tang G., Zhao H., Wu J., Zhang, Y. Optimization of braking force distribution for three-axle truck. SAE Technical Paper 2013-01-0414, 2013. https://doi.org/10.4271/2013-01-0414
7. Limpert R. An investigation of the brake force distribution on tractor-semitrailer combinations. SAE Technical Paper 710044 1971. https://doi.org/10.4271/710044
8. Zheng H., Liu C., Wang L. A braking force distribution strategy in integrated braking system based on wear control and hitch force control. SAE Technical Paper 2018-01-0827, 2018. https://doi.org/10.4271/2018-01-0827
9. Beyer C., Schramm H., Wrede, J. Electronic braking system EBS - status and advanced functions. SAE Technical Paper 982781, 1998. https://doi.org/10.4271/982781
10. Nakazawa M., Isobe O., Takahashi S., Watanabe Y. Braking force distribution control for improved vehicle dynamics and brake performance. Vehicle System Dynamics 1995; 24 (4-5): 413-426. https://doi.org/10.1080/00423119508969101
11. Wabco. Pneumatic braking system. Agriculture and forestry. Product catalogue 2017. https://www.wabco-customercentre.com/catalog/docs/8150100823.pdf
12. Forrer P. Brake systems in agricultural and forestry vehicles. https://www.laumetris.lt/UserFiles/image/downloads/Dual_and_Single_Line_Hydraulic_Brakes_Paul_Forrer_EN.pdf
13. Miatluk M, Kamiński Z. Układy hamulcowe pojazdów. Obliczenia. Wydawnictwo Politechniki Białostockiej, 2005.
14. Sun, B., Wang, P., Gao, S., Yu, J., Wang, Z. Development of braking force distribution strategy for dual-motor-drive electric vehicle. Journal of Engineering and Technological Sciences 2018; 50(2): 179-201. https://doi.org/10.5614/j.eng.technol.sci.2018.50.2.3
15. Li X., Zhang X., Wang Y. Regenerative braking control strategies with fixed ratio and variable ratio braking forces optimization distribution for electric vehicles during downhill process. International Journal of Automotive Technology 2022; 23: 667-681. https://doi.org/10.1007/s12239-022-0061-7
16. Limpert, R. Brake design and safety (3rd ed). SAE International, 2011. https://doi.org/10.4271/R-398
17. Harwood D.W. Review of Truck Characteristics as Factors in Roadway Design. The National Academies Press, 2003. https://doi.org/10.17226/23379
18. Stegherr H., Heider M. Hähner, J. Classifying metaheuristics: towards a unified multi-level classification system. Natural Computing 2022; 21(2): 155-171. https://doi.org/10.1007/s11047-020-09824-0
19. Tomar V, Bansal M, Singh P. Metaheuristic algorithms for optimization: a brief review. Engineering Proceedings 2023; 59(1): 238. https://doi.org/10.3390/engproc2023059238
20. Hamadneh T., Batiha B., Werner F., Eguchi K.,

Montazeri Z., Dehghani M. A completely different and innovative bio-inspired metaheuristic approach for effectively solving complex optimization problems across various domains. Preprints 2024; 2024091803. https://doi.org/10.20944/preprints202409.1803.v1

21. Rahimi I., Gandomi A.H., Chen F. et al. A Review on constraint handling techniques for population-based algorithms: from single-objective to multi-objective optimization. Archives of Computational Methods in Engineering 2023; 30(3): 2181–2209. https://doi.org/10.1007/s11831-022-09859-9
22. Oztas G.Z., Erdem S. A penalty-based algorithm proposal for engineering optimization problems. Neural Computing and Application 2023; 35(10): 7635–7658. https://doi.org/10.1007/s00521-022-08058-8
23. Kasem M. A. M., Maalawi K. Efficient algorithms and models for mechanical and structural design optimization. Journal of Mechanical Engineering and Sciences 2021; 15(3): 8405–8417. https://doi.org/10.15282/jmes.15.3.2021.17.0661
24. Haataja M., Leinonen, T. On the distribution of braking forces in road braking. SAE Technical Paper 2000-01-3413 2000. https://doi.org/10.4271/2000-01-3413
25. Liu Z., Zheng H., Xu W. A model-based mass estimation and optimal braking force distribution algorithm of tractor and semi-trailer combination. SAE Technical Paper 2013-01-0418 2013. https://doi.org/10.4271/2013-01-0418
26. Zhang N., Wu J., Li T., Zhao Z., Yin G. Influence of braking on dynamic stability of car-trailer combinations. Proceedings of the Institution of Mechanical Engineers, Part D: Journal of Automobile Engineering 2021; 235(2-3): 455-464. doi:10.1177/0954407020959895
27. Radlinski R.W., Wiliams S.F. NHTSA heavy duty vehicle brake research program: Report no. 1 - stopping capability of air braked vehicles. National Highway Traffic Safety Administration, 1985.
28. BPW. Mechanical load-dependent brake force regulator. The unique solution for the requirements imposed by regulation EU 2015/68. https://bpwagrar.comen/mlb/
29. Schlueter M., Gerdts M., Rueckmann J.J. A numerical study of MIDACO on 100 MINLP benchmarks. Optimization 2012; 61(7): 873-900, https://doi.org/10.1080/02331934.2012.668545
30. 30. Schlueter M., Gerdts M. The oracle penalty method. Journal of Global Optimization 2010; 47(2): 293-325. https://doi.org/10.1007/s10898-009-9477-0
31. MIDACO-SOLVER. Numerical high-performance optimization Software. http://www.midaco-solver.com/
32. Yang X.S., Deb S. Engineering optimisation by Cuckoo Search. International Journal of Mathematical Modelling and Numerical Optimisation 2010; 1(4): 330-343. https://doi.org/10.1504/IJMMNO.2010.035430
33. Yang, X.-S. Nature-inspired optimization algorithms (2nd ed.). Elsevier, 2020.
34. Yang X.-S. Nature-inspired metaheuristic algorithm. Luniver Press, 2010.
35. Kirkpatrick S., Gelatt C.D., Vecchi, M.P. Optimization by simulated annealing. Science 1983; 220(4598): 671-680. http://dx.doi.org/10.1126/science.2204598.671
36. Yang X.-S. Cuckoo Search (CS) algorithm (https://www.mathworks.com/matlabcentral/fileexchange/29809-cuckoo-search-cs-algorithm). MATLAB Central File Exchange, 2024.
37. Yang X.-S. Firefly Algorithm (https://www.mathworks.com/matlabcentral/fileexchange/29693-firefly-algorithm). MATLAB Central File Exchange, 2024.
38. Yang X.-S. Simulated annealing for constrained optimization (https://www.mathworks.com/matlabcentral/fileexchange/29739-simulated-annealing-for-constrained-optimization). MATLAB Central File Exchange, 2024.
39. Geem, Z.W., Kim J.H., Loganathan G.V. A new heuristic optimization algorithm: Harmony search. Simulation 2001; 76 (2): 60–68. https://doi.org/10.1177/003754970107600201
40. Fesanghary M. Harmony Search Algorithm (https://www.mathworks.com/matlabcentral/fileexchange/28850-harmony-search-algorithm), MATLAB Central File Exchange, 2024.
41. Kroese D.P., Taimre T., Botev Z.I. Handbook of Monte Carlo methods. John Wiley and Sons, 2011.
42. Kamiński Z. Calculation of the optimal braking force distribution in three-axle trailers with tandem suspension. Acta Mechanica et Automatica 2022; 16(3): 189-199. https://doi.org/10.2478/ama-2022-0023
43. Burkhardt, J. Various software. MATLAB source codes. The Hammersley Quasi Monte Carlo (QMC) Sequence 2020. https://people.sc.fsu.edu/~jburkardt/m_src/hammersley/hammersley.html
44. Hammersley J. M. Monte Carlo methods for solving multivariable problems. Annals of the New York Academy of Sciences 1960; 86(3): 844-874. https://doi.org/10.1111/j.1749-6632.1960.tb42846.x
45. Bryant D., Day A. Braking of Road Vehicles. Elsevier, 2022. https://doi.org/10.1016/C2019-0-04185-4
46. Revised standards for agricultural vehicles. RSA Guide. Road Safety Authority, 2015.
47. ISO 8855: 2011. Road vehicles - Vehicle dynamics and road-holding ability-Vocabulary.
48. BPW agricultural catalogue. Growing together. Customised solutions, 2020.
49. https://www.bpw.de/fileadmin/data/downloads/BPW_Agricultural_Catalogue_2020_en.pdf
50. Colaert Essieux. General catalogue, 2023. https://www.adraxles.com/gallery/catalogue-colaert-essieux-2023-v22-11-18-lr.pdf